The Subaru Coronagraphic Extreme AO Project

Frantz Martinache[a] and Olivier Guyon[a]

[a]Subaru Telescope, 650 N. A'ohoku Place, HI 96720, USA

ABSTRACT

The Subaru Coronagraphic Extreme AO (SCExAO) Project is an upgrade to the newly commissioned coronagraphic imager HiCIAO for the Subaru Telescope, in the context of a massive survey for exoplanets and disks called SEEDS. SCExAO combines a high-performance coronagraph PIAA coronagraph and non-redundant aperture masking interferometry to a MEMS-based wavefront control system to be used in addition to the 188-actuator Subaru Adaptive Optics (AO188) system. The upgrade is designed as a flexible platform with easy access to both pupil and image planes to allow quick implementation of new high-angular resolution techniques, using a combination of interferometry and coronagraphy. The SCExAO system will enhance SEEDS by offering access to smaller separations and improved PSF calibration, and will therefore allow high quality follow-up observations of challenging SEEDS candidates. SCExAO will also enable new science investigations requiring high contrast imaging of the innermost (< 0.2 arc second) surrounding of stars.

1. INTRODUCTION

The validation of planet formation scenarios and evolutionary theories requires the identification of a large population of young planetary systems whose orbital and atmospheric properties can be directly measured, independently of the use of a model. Conventional AO observations and the use of the successful Angular Differential Imaging (ADI) technique that led to the discovery of the HR 8799 system on Gemini and Keck[1] can only efficiently probe for objects at angular separations greater than 0.5 arc second and reach maximum sensitivity around 1 arc second (current HiCIAO performance estimate respectively give contrasts of 9.5 and 12 magnitudes for separations of 0.5 and 1 arc second respectively on a m_V=6 star).

Even for the nearest populations of young stars, at distances of 30 pc, the current AO performance translates into projected orbital separations greater than 30 AU. While some potentially planetary mass objects do seem to form at such large radii, RV surveys and the structure of our own Solar system suggest that most planet formation occurs at a smaller separation. Moreover, for most of the directly imaged extrasolar planet candidates, orbital periods are too long to allow significant orbital coverage,[2,3] which would lead to dynamical masses, a most important piece of information in the puzzle of planet formation. The planetary status of such candidates remains model-dependent and in some cases controversial.

The Subaru Coronagraphic Extreme AO (SCExAO) project was designed to palliate this flaw and implements the necessary techniques to probe the innermost parts of extrasolar planetary systems, providing access to their habitable zone. The SCExAO project benefits from the most recent developments in coronagraphy, interferometry and advanced wavefront control techniques, many of which have been pioneered by our group at Subaru. It builds upon recent successful developments at Subaru Telescope: the AO188 Adaptive Optics system and the coronagraphic imager HiCIAO.[4] SCExAO's access to small angular separations and its location in the Northern hemisphere make it scientifically complementary to ESO's SPHERE and Gemini's GPI projects. The flexible layout of SCExAO allows use of high performance techniques which were not available when SPHERE and GPI were designed, and continuous upgrades of the system will keep SCExAO competitive for the next decade.

SCExAO is designed as a flexible, easy access platform providing access to both image and pupil plan to welcome guest coronagraphs and attractive wavefront control schemes. A MEMS-type deformable mirror will allow active speckle calibration without relying on expected planet properties (spectral differential imaging). For the its first version, currently being assembled in the Subaru simulation lab, the choice of a Phase Induced Amplitude Apodization (PIAA) Coronagraph and the implementation of non-redundant aperture masking interferometry (NRM) make of SCExAO the instrument that will provide the best inner working angle (respectively 40 and 20 mas) of the coming generation of ground based planet finders on the 8 to 10 meter class telescopes.

email: frantz@naoj.org

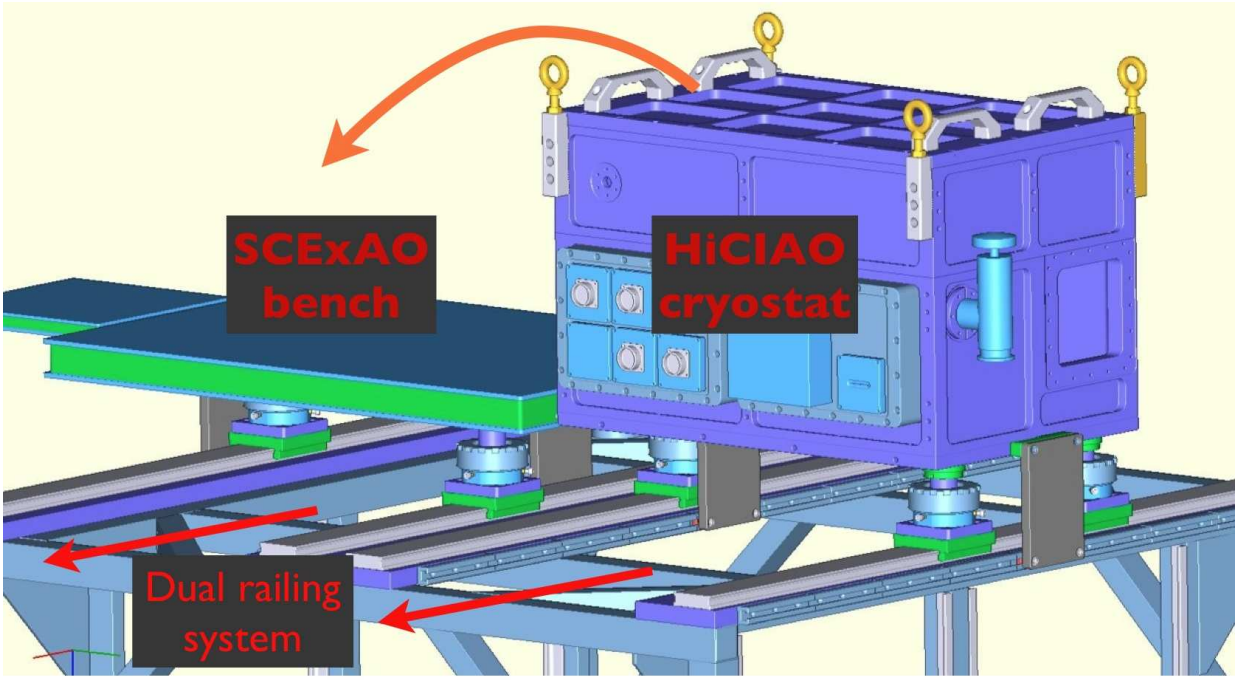

Figure 1. CAD drawing of the SCExAO frame. On this drawing, the light comes from the far left (AO side) and travels to the right toward HiCIAO. The top of this new frame incorporates a twin railing system that provides good lateral flexibility in the positioning of the elements of the AO188-SCExAO-HiCIAO chain. To exactly reproduce the current observing mode of HiCIAO, the lightweight SCExAO bench (on the left) can be taken off the frame and HiCIAO moved to the front position (bent arrow).

2. OPTO-MECHANICAL DESIGN

SCExAO was conceived as an upgrade of the coronagraphic fore-optics currently in front of HiCIAO, stationed on the Subaru Telescope IR Nasmyth platform. In order not to impact the current observing modes of HiCIAO, a new frame was designed to accomodate both the current (fore-optics + HiCIAO) and new (SCExAO + HiCIAO) observing configurations. Figure 1 shows a CAD view of this frame whose delivery at the telescope is scheduled for January 2010.

The SCExAO bench is built from a 1.2-meter long optical table. Figure 2 maps the location of the SCExAO optics on this table. As it travels from left to right on the drawing, the light coming from the AO188 is reflected once by a field flat mirror, and then a second time by the 1024-actuator MEMS DM, located in a divergent beam, before being collimated. The beam is then shaped using a unique set of optics: the SRP[5] that suppresses the spider vanes (c.f. Section 3.1) and the PIAA[6–10] that apodizes the beam and suppresses the central obscuration (c.f. Section 3.2). In the following focal plane, the light of an on-axis source is reflected by an annular mask onto the coronagraphic low-order wavefront sensor[11] (c.f Section 4). The light of other sources goes to the left where the beam is de-apodized by the inverse PIAA (c.f. Section 5), to recover "wide-field" of view capability. To probe the innermost part of the target systems (down to 0.5 λ/D), a non-redundant aperture mask[12,13] is located in the output pupil plan, before getting inside the HiCIAO cryostat.

3. LOSSLESS APODIZATION

3.1 Spider Removal Plate

Because it is designed to accomodate prime focus instruments, the spider vanes of the Subaru Telescope are fairly thick (224 mm), even relative to the 7.92 m pupil diameter. If left uncorrected, they create four intense diffraction spikes at the $\sim 10^3$ contrast level. To suppress this diffraction, our approach is to translate each of the four parts of the beam with a single tilted plate of glass to fill the spider gap. The SRP (Spider Removal

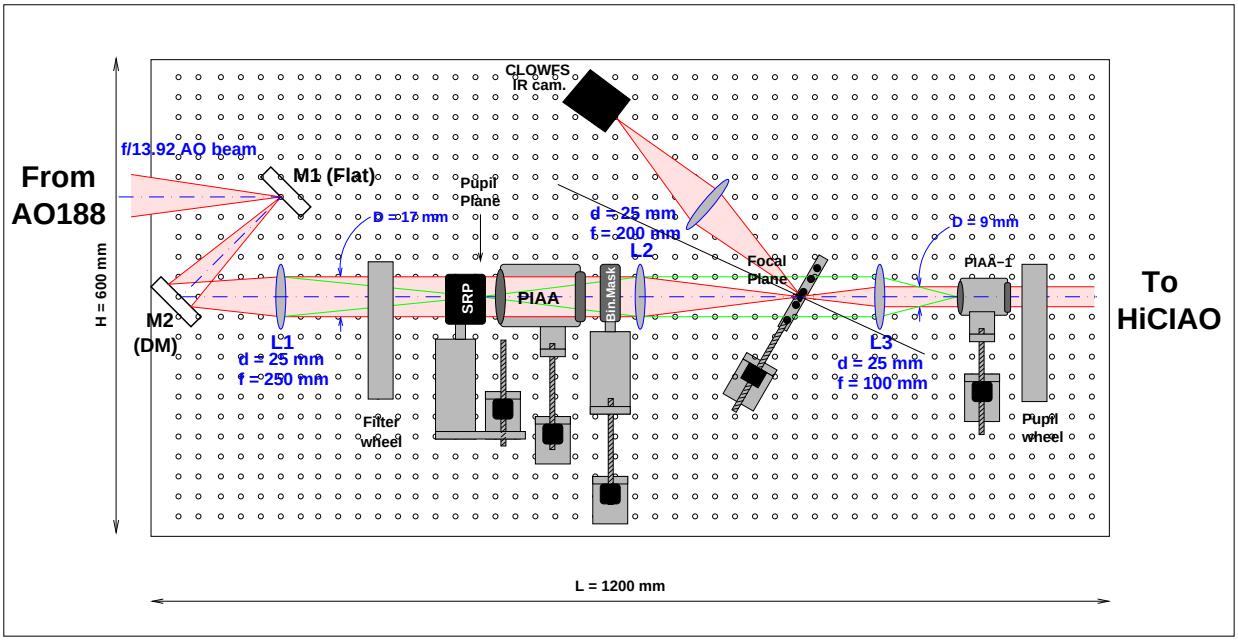

Figure 2. Optical design of the SCExAO bench. The light travels from the left (AO188 side) to the right (HiCIAO side), bounces off the DM located in a divergent beam, and is collimated before being shaped by the SRP and the hybrid PIAA, for high contrast coronagraphy. The focal plane mask reflects part of the on-axis source light toward the Coronagraphic Low-Order Wavefront Sensor camera. Anything else reaches the science camera HiCIAO after being de-apodized by the inverse PIAA.

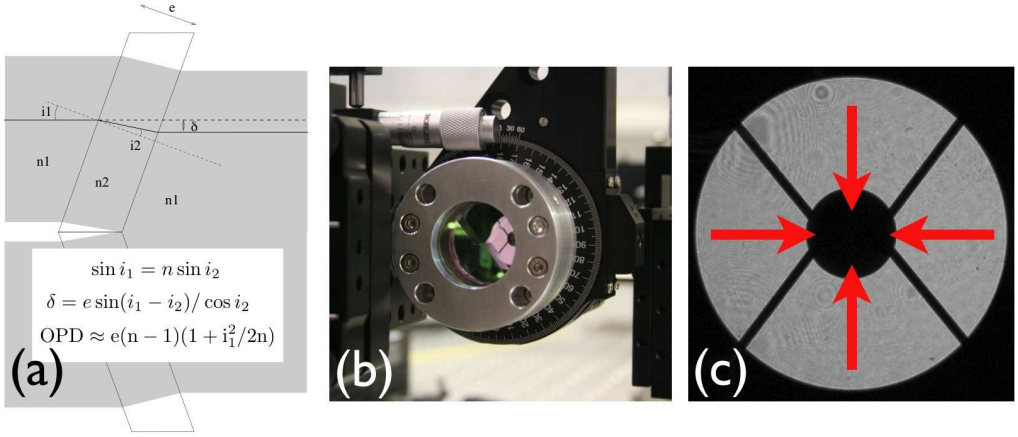

Figure 3. Suppression of the spider vanes by the Spider Removal Plate. While simple geometric optics principles (panel a) explain its machinery, the actual 3D geometry (panel b) is non-trivial due to the peculiar Subaru spider vanes geometry. Nevertheless, the SRP successfully translates the four quadrants of the pupil (panel c) inward, significantly reducing the diffraction by the spider vanes.

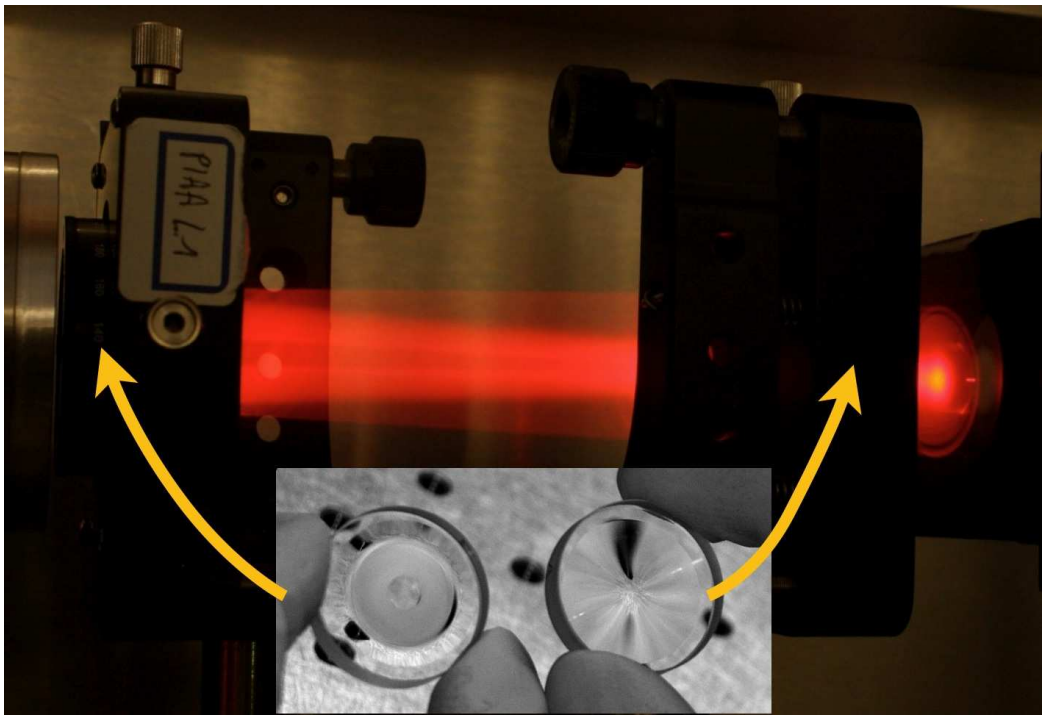

Figure 4. Apodization of the beam by the the PIAA lenses, a core component of the SCExAO bench. The lens L_1 (on the left), changes the distribution of light in the pupil plane and L_2 (on the right) compensates for the distorsions of the wavefront L_1 introduces. Notice that as the light travels from L_1 to L_2, the central obscuration of the telescope disappears and the pupil becomes apodized.

Plate) consists of four tilted plane-parallel plates, each tranlating a part of the pupil inwards, as shown in Fig. 3. All plates were cut from the same plate-parallel plate (a.k.a. optical window), to guarantee within tolerances, a constant thickness. For a window of thickness $e = 15$ mm of refractive index n =1.443 (fused silica for $\lambda = 1.6$ μm), each plate needs to be tilted by an angle $\alpha = 5.004 \pm 0.02°$, to guarantee the continuity of the wavefront on-axis after remapping within $\lambda/10$.

3.2 PIAA for centrally obstructed telescope

The simplest way of performing an apodization is to insert a mask with a radial transmission profile that follows a prolate spheroidal function, the so-called classical pupil apodization (CPA). While extremely robust, and insensitive to moderate tip-tilt residuals, this approach has two main drawbacks: the throughput is low (as low as ~ 0.1 for a 10^{-10} contrast[14]), and the effective pupil diameter is reduced by a factor approximately equal to the square root of the throughput (due to the fact that apodizers remove the light mostly at the edges of the pupil), which translates into a loss of angular resolution.

The PIAA[6] addresses these issues and apodizes the beam using a very different approach. It uses a set of two aspheric optics working as a pair. Inserted in the pupil plane, the first (L_1 on Figure 4) changes the distribution of light, while the second (L_2) collimates the beam for an on-axis source. The design retained for the SCExAO upgrade (cf. Figure 4) suppresses the central obscuration. Unlike CPA that discards light, the PIAA redistributes it across the pupil and therefore preserves the throughput and the angular resolution. Its main drawback is however the introduction of large aberrations for off-axis sources, which will be corrected by the inverse PIAA discussed in Section 5.

3.3 Beam shaping

Figure 5 shows a picture of these beam-shaping elements forming a very compact module on the SCExAO bench. All these elements are mounted on motorized translation stages and can be individually driven in and out of the

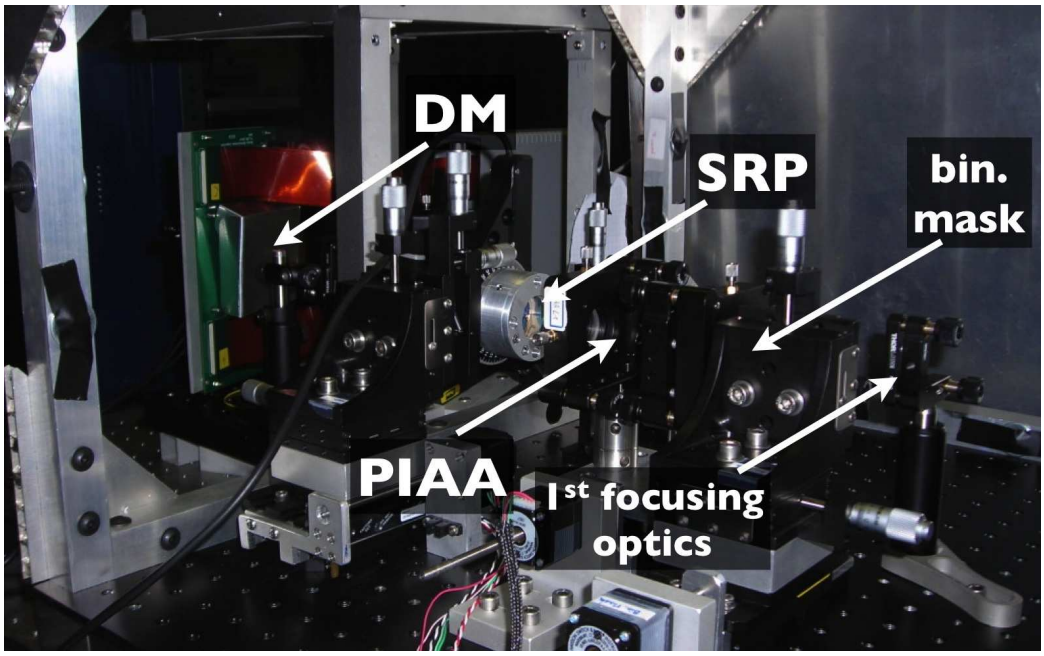

Figure 5. Close-up on the beam shaping module of the SCExAO bench. After the additional wavefront correction by the DM, the SRP, PIAA and binary mask apodize the beam for optimal coronagraphy of the star in the following focal plane. Note that all these elements are mounted on motorized stages and can be driven in and out of the beam by the SCExAO main computer.

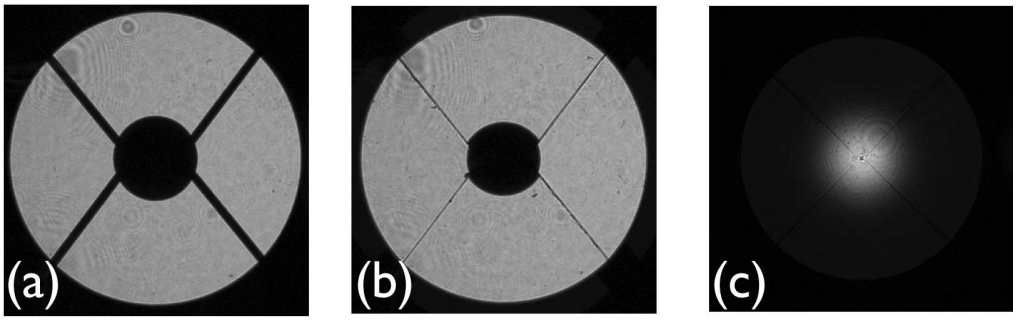

Figure 6. The different stages of the beam apodization: the original Subaru pupil before beam shaping (panel a), after the SRP (panel b) and after the PIAA (panel c).

beam for quick diagnostic. Figure 6 demonstrates the interest of this capability by showing the different steps of the shaping of the beam: SRP and PIAA.

4. LOW-ORDER WAVEFRONT SENSOR

Because it is optimized for the detection of companions at low angular separations, a high-performance coronagraph such as the PIAA is pushed to become highly sensitive to low-order aberrations, and especially pointing errors. Indeed, for angular separations close to 1 λ/D, the signal created by a small ($<< \lambda/D$) pointing error can perfectly mimic the one of a high-contrast companion that would be located at a larger separation. Since the coronagraph is designed to transmit the signal of such companions, it will transmit the pointing error signal. The SCExAO system therefore includes a robust and accurate wavefront sensor to measure the tip-tilt as well as defocus, so-called Coronagraphic Low-Order Wavefront Sensor (CLOWFS).

CLOWFS uses the light reflected by the focal plane mask located after the apodizer (c.f. Figure 7). However, instead of reflecting all the on-axis stellar light, the central part of the mask is opaque and only a reflective

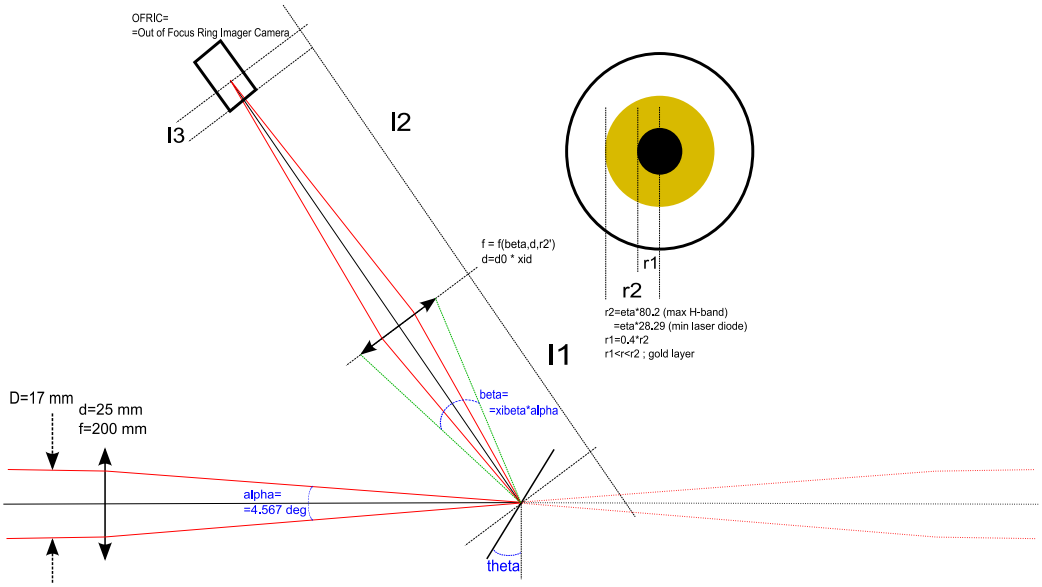

Figure 7. Principle of the Coronagraphic Low Order Wavefront Sensor. The CLOWFS camera (top left of the image) acquires a defocused image of a reflective ring-shaped fraction of the focal plane occulting mask. The light of other off-axis sources travels to the right, toward HiCIAO.

annulus around this central part sends light to the CLOWFS camera, which acquires a defocused image of this annulus.[11] Discarding the central part of the light rejects a lot of flux that contains very little signal. In a manner that is reminiscent of Schlieren photography or the Foucault knife-edge, this central dark zone makes tiny changes in the wavefront produce macroscopic changes in the CLOWFS image.[11] For wavefront aberrations smaller than 1 radian, the CLOWFS image is a linear function of the wavefront aberration modes. In the lab,[11] CLOWFS has demonstrated very good performance, successfully helping to stabilize the tip-tilt with residuals approaching $10^{-3}\lambda/D$.

5. INVERSE PIAA

As described in Section 3.2 and in Figure 4, the PIAA is made of two lenses, which remap the light and maintain a flat wavefront for an on-axis source. For an off-axis source, the remapping the PIAA performs introduces aberrations, and the corresponding diffraction pattern changes as a function of the off-axis. Figure 8 demonstrates this property of PIAA. Because it is not only designed to apodize the beam but also to fill the gap left by the central obscuration, the SCExAO PIAA produces some very unusual pineapple-shaped off-axis diffraction patterns. Since the original publication of the concept,[6] it has been suggested that an exact copy of the PIAA, located in a pseudo-pupil plane after the coronagraphic mask and plugged backwards, should cancel these aberrations. The SCExAO system is the first experiment to successfully implement such an inverse system. A comparison of the three rows of images presented in Figure 8 will convince the reader that the inverse system efficiently corrects the huge off-axis aberrations the PIAA introduces in the first place (middle row), and turns the pineapple-shaped diffraction patterns back into conventional Airy-like images (bottom row), virtually identical to the images the system produces with no apodization at all (top row).

6. SYSTEM PERFORMANCE IN PHASE 1

The first installment of the SCExAO system at the Subaru Telescope is scheduled for January 2010, with the delivery of a frame that can carry the SCExAO bench, HiCIAO as well as other guest instruments which would benefit from the capabilities of SCExAO. The absence of a fast wavefront sensor in this first "phase-1" installment will prevent the system from running in extreme-AO mode. The 1024-actuator MEMS deformable mirror (DM) in place in the system will however be used:

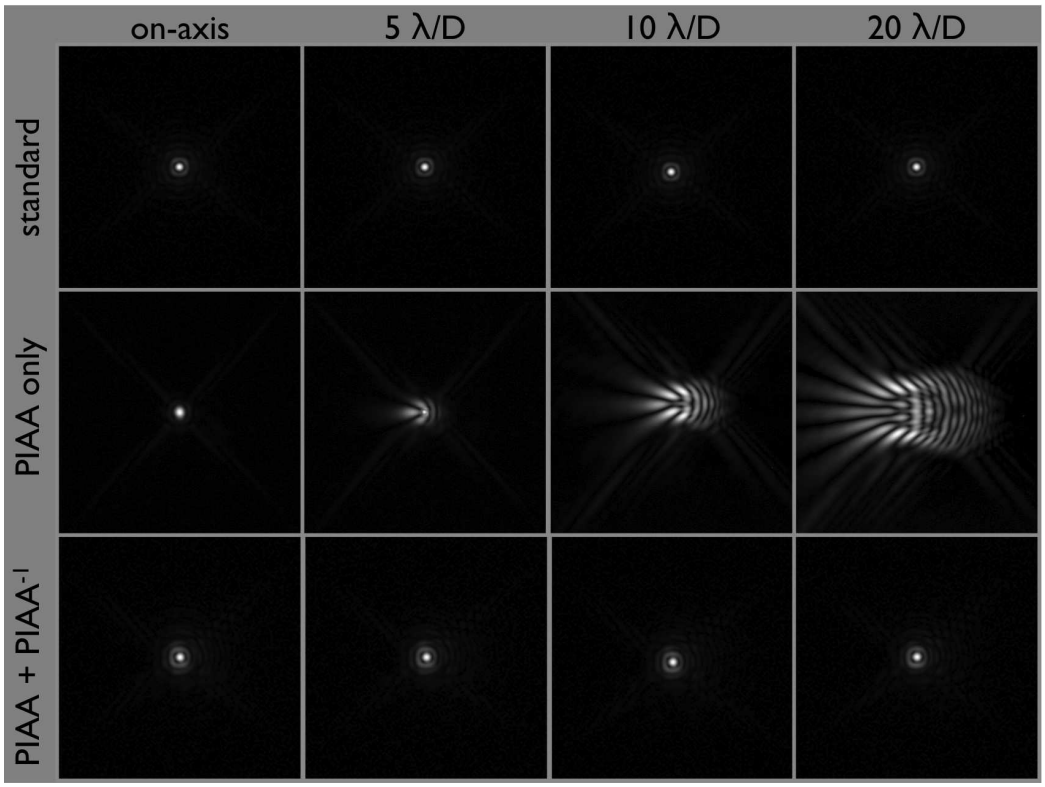

Figure 8. Effect of the inverse PIAA system. The images of three different optical configurations are shown. From top to bottom: no apodization, PIAA only and PIAA + inverse PIAA.

- to cancel out the non-common path errors responsible for the presence of quasi-static and slowly moving speckles in a preliminary calibration procedure using phase diversity
- to calibrate the speckles by measuring their coherence. While observing, the DM can be used to actively probe the coherence of the speckles which will distinguish them from potential companions.

The efficiency of this latter technique was validated in a lab experiment at the 3.510^{-9} contrast level,[15] that is more than three orders of magnitude deeper in contrast than what can be achieved from the ground. Expected performance of the SCExAO system in "phase 1" is plotted on Figure 9. The yellow curve is the current HiCIAO detection limit (private communication) extrapolated to a 1 hour observing time. For angular separations smaller than 0.5 arc seconds (cut-off frequency of the DM), SCExAO will outperform the ADI contrast by a factor 10.

REFERENCES

[1] Marois, C., Macintosh, B., Barman, T., Zuckerman, B., Song, I., Patience, J., Lafrenière, D., and Doyon, R., "Direct Imaging of Multiple Planets Orbiting the Star HR 8799," *Science* **322**, 1348– (Nov. 2008).

[2] Neuhäuser, R., Guenther, E. W., Wuchterl, G., Mugrauer, M., Bedalov, A., and Hauschildt, P. H., "Evidence for a co-moving sub-stellar companion of GQ Lup," *A&A* **435**, L13–L16 (May 2005).

[3] Chauvin, G., Lagrange, A.-M., Zuckerman, B., Dumas, C., Mouillet, D., Song, I., Beuzit, J.-L., Lowrance, P., and Bessell, M. S., "A companion to AB Pic at the planet/brown dwarf boundary," *A&A* **438**, L29–L32 (Aug. 2005).

[4] Hodapp, K. W., Suzuki, R., Tamura, M., Abe, L., Suto, H., Kandori, R., Morino, J., Nishimura, T., Takami, H., Guyon, O., Jacobson, S., Stahlberger, V., Yamada, H., Shelton, R., Hashimoto, J., Tavrov, A., Nishikawa, J., Ukita, N., Izumiura, H., Hayashi, M., Nakajima, T., Yamada, T., and Usuda, T., "HiCIAO:

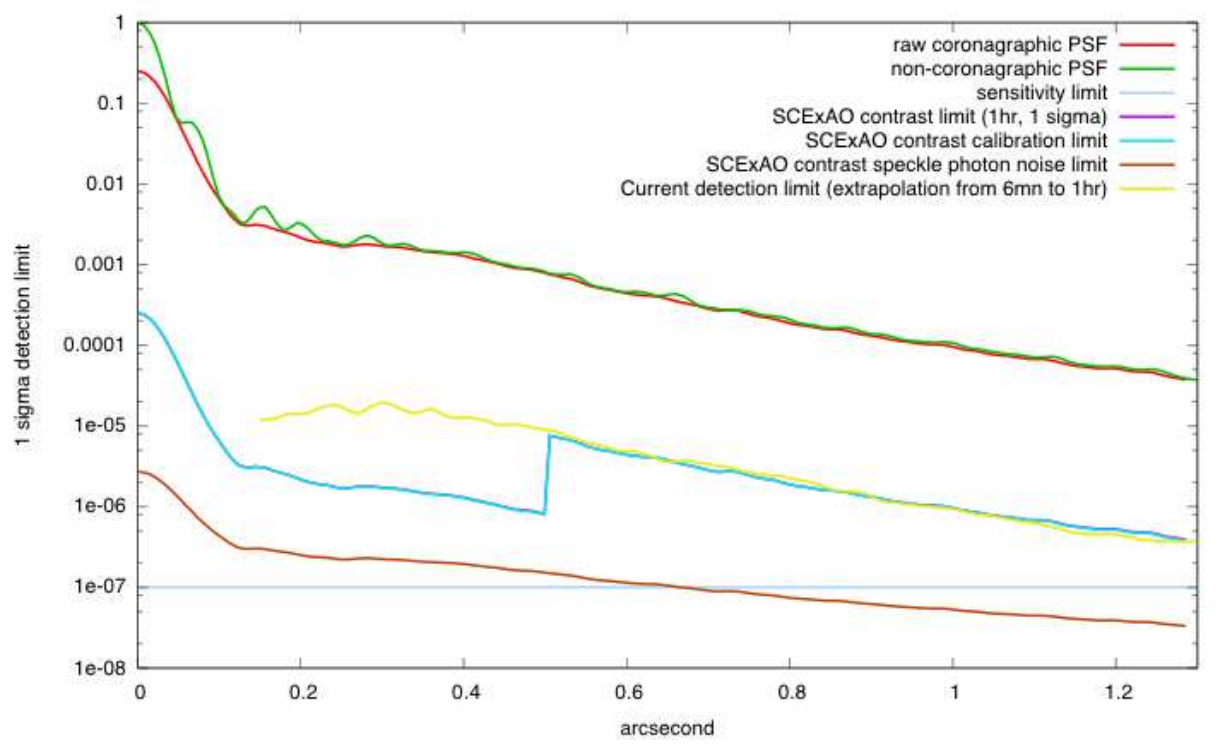

Figure 9. SCExAO performance while in phase 1 (i.e. non extreme-AO mode). The calibration of the speckle coherence improves the coronagraphic PSF by a factor $\sim 10^3$, for angular separations smaller than 0.5 arc seconds.

the Subaru Telescope's new high-contrast coronographic imager for adaptive optics," in [*Society of Photo-Optical Instrumentation Engineers (SPIE) Conference Series*], *Society of Photo-Optical Instrumentation Engineers (SPIE) Conference Series* **7014** (Aug. 2008).

[5] Lozi, J., Martinache, F., and Guyon, O., "Phase-Induced Amplitude Apodization on centrally obscured pupils: design and first laboratory demonstration for the Subaru Telescope pupil," *ArXiv e-prints* (Mar. 2009).

[6] Guyon, O., "Phase-induced amplitude apodization of telescope pupils for extrasolar terrestrial planet imaging," *A&A* **404**, 379–387 (June 2003).

[7] Guyon, O., Pluzhnik, E. A., Galicher, R., Martinache, F., Ridgway, S. T., and Woodruff, R. A., "Exoplanet Imaging with a Phase-induced Amplitude Apodization Coronagraph. I. Principle," *ApJ* **622**, 744–758 (Mar. 2005).

[8] Martinache, F. and Guyon, O., "Performance of a Phase Induced Amplitude Apodization Coronograph," in [*EAS Publications Series*], Carbillet, M., Ferrari, A., and Aime, C., eds., *EAS Publications Series* **22**, 281–289 (2006).

[9] Martinache, F., Guyon, O., Pluzhnik, E. A., Galicher, R., and Ridgway, S. T., "Exoplanet Imaging with a Phase-induced Amplitude Apodization Coronograph. II. Performance," *ApJ* **639**, 1129–1137 (Mar. 2006).

[10] Pluzhnik, E. A., Guyon, O., Ridgway, S. T., Martinache, F., Woodruff, R. A., Blain, C., and Galicher, R., "Exoplanet Imaging with a Phase-induced Amplitude Apodization Coronagraph. III. Diffraction Effects and Coronagraph Design," *ApJ* **644**, 1246–1257 (June 2006).

[11] Guyon, O., Matsuo, T., and Angel, R., "Coronagraphic Low-Order Wave-Front Sensor: Principle and Application to a Phase-Induced Amplitude Coronagraph," *ApJ* **693**, 75–84 (Mar. 2009).

[12] Martinache, F., Rojas-Ayala, B., Ireland, M. J., Lloyd, J. P., and Tuthill, P. G., "Visual Orbit of the Low-Mass Binary GJ 164 AB," *ApJ* **695**, 1183–1190 (Apr. 2009).

[13] Martinache, F., Guyon, O., and Garrel, V., "Aperture Masking Interferometry for Subaru," *ArXiv e-prints* (May 2009).

[14] Guyon, O., Pluzhnik, E. A., Kuchner, M. J., Collins, B., and Ridgway, S. T., "Theoretical Limits on Extrasolar Terrestrial Planet Detection with Coronagraphs," *ApJS* **167**, 81–99 (Nov. 2006).

[15] Guyon, O., Pluzhnik, E. A., Martinache, F., Totems, J., Tanaka, S., Matsuo, T., Blain, C., and Belikov, R., "High Contrast Imaging and Wavefront Control with a PIAA Coronagraph: Laboratory System Validation," *PASP* **submitted** (2009).